Scaled Quantum Chemical Calculations and FT-IR, FT- Raman Spectral Analysis of 4-Hydroxy-3-Nitrocoumarin

M. Sivasubramanian
Professor in Physics,
Unnamalai Institute of Technology,
Kovilpatti – 628 502, Thoothukudi District, Tamil Nadu, India

Abstract

FT-IR and FT-Raman spectra of 4-Hydroxy-3-Nitrocoumarin have been recorded in the range of 4000–400 cm^{-1} and 4000–10 cm^{-1} respectively. A detailed vibrational analysis have been carried out and assignments of the observed fundamental bands have been proposed on the basis of peak positions, relative intensities, fundamentals, overtones and combination bands. With the hope of providing more and effective information on the fundamental vibrations, Density Functional Theory (DFT)-Beck3-Lee-Yang-Parr(B3LYP) levels with 6-31G basis set have been employed in quantum chemical analysis and normal coordinate analysis has been performed on 4-Hydroxy-3-Nitrocoumarin, by assuming Cs point group symmetry. The computational wavenumbers are in good agreement with the observed results. The theoretical spectra obtained agree well with the observed spectra.*

KEYWORDS: ***4-Hydroxy-3-Nitrocoumarin; FT-IR; FT-Raman; Density functional theory calculations; wavenumbers***

1. Introduction

Coumarin derivatives are associated with the class of naturally occurring lactones that are found in different food sources, such as fruits, herbs, and vegetables[1]. The chemical name of coumarin is benzopyrone. Several naturally occurring coumarin derivatives have considerable interest in terms of biological and potential drugs. The pharmacological activity of many coumarin derivatives has been extensively investigated [2-9]. 3-Alkyl and 4-alkyl coumarins are known to posses various physiological activities[10,11] and 4-arylisocoumarins posses antialergic property[12]. Some coumarin derivatives found to have anti cancer [13,14], diuretic, analgesic, myorelaxant [15], antifungal [16] and anthelmintic [17] activities. Coumarin derivatives having sulphonamide moiety are found to have antimicrobial [18,19], antifungal [20], antitubercular [21] activities and anti-tumor promoting effect [22].

When ingested, coumarin acts as a blood thinner. Coumarin 153 is useful to test the reliability of dielectric continuum model for estimating dielectric friction effect [23]. Also, coumarin and its derivatives are important for the synthesis of many oxygen heterocyclics and pyrazoles. Heterocyclic ring fused on substituted coumarins has become an attractive target in organic synthesis because of their significance in biological systems. Thus, coumarin derivatives are subject of considerable pharmaceutical and chemical interest. In recent years, much of the attention has been focused mainly on the coumarin synthesis and identification [24-33]. Consideration of all these factors led to undertake a detailed Infrared and Raman spectral studies and vibrational assignments of 4-Hydroxy-3-Nitrocoumarin.

The vibrational wavenumbers obtained by quantum chemical calculations are typically larger than their experimental counterparts [34] and they have to be scaled by empirical scaling factors ranging from 0.801 to 0.996. These scaling factors are determined from the mean deviation between the calculated and experimental wavenumbers [35-37]. The aim of this work is to predict the vibrational spectra of 4-Hydroxy-3-Nitrocoumarin by applying the density functional theory (DFT) calculations based on Becke3-Lee-Yang-Parr (B3LYP) level with the use of the standard 6-31G* basis set. The calculated vibrational wavenumbers were compared with the experimental results obtained and the simulated and observed spectra were also analyzed in detail.

2. Experimental Details

Spectroscopically fine samples of 4-Hydroxy-3-Nitrocoumarin is obtained from Lancaster Chemical Company, UK, and used as such without further purification for the spectral measurements. The room temperature Fourier transform infrared spectum of the title compound is measured in the region 4000–400 cm^{-1}, at a resolution of ±1 cm^{-1}, using BRUCKER IFS 66V vacuum Fourier transform spectrometer, equipped with an MCT detector, a KBr beam splitter and globar source. Fourier transform Raman spectrum of the title compound is measured in the range of 4000 – 10 cm^{-1}, using Bruker RFS 100/S FT-Raman spectrometer.

3. Computational Details

Density functional theory calculation was carried out by means of the 2003 version of the GAUSSIAN suit of program package [38] with B3LYP level using the standard 6-31G* basis set [39,40]. The normal grid (50,194) was used for numerical integration. The Cartesian representation of the theoretical force constants has been computed at the fully optimized geometry by assuming Cs point group symmetry. Scaling of the force fields were performed by the scaled quantum mechanical (SQM) procedure.

$$F_{ij}^{scaled} = (c_i c_j)^{1/2} F_{ij}^{B3LYP} \quad .....(1)$$

Where C_i is the scale factor of coordinate i, F_{ij}^{B3LYP} is the B3LYP/6-31G* force constant in the local internal coordinates, and F_{ij}^{scaled} is the scaled force constant. The multiple scaling of the force constants was performed by the quantum chemical method with selective scaling in the local symmetry coordinate representation [41] using transferable scale factors available in the literature [42]. The transformation of force field from Cartesian to symmetry coordinate, the scaling, the subsequent normal coordinate analysis, calculations of total energy distribution (TED), IR and Raman intensities were done on a PC with the version V7.0-G77 of the MOLVIB program written by Sundius [43,44]. To achieve a close agreement between observed and calculated, the least square fit refinement algorithm was used to recalculate the normal modes, TED and the corresponding theoretically expected IR intensities.

The prediction of Raman intensities was carried out by following the procedure outlined below. The Raman activities (S_i) calculated by the Gaussian–2003 program and adjusted during scaling procedure with Molvib were converted to relative Raman intensities (I_i) using the following relationship derived from the basic theory of Raman scattering.

$$I_i = \frac{f(\upsilon_o - \upsilon_i)^4 S_i}{\upsilon_i \left[1 - \exp(-hc\upsilon_i / kT)\right]} \quad .....(2)$$

Where υ_0 is the exciting frequency, and υ_i is the vibrational frequency of the i^{th} normal mode, h, c and k are fundamental constants, and f is a suitably chosen common normalization factor for all peak intensities.

4. Results and Discussion

4.1. Molecular structure and symmetry

The bond lengths and bond angles calculated by means of B3LYP method for the title compound is depicted in Table 1.

Table 1 Optimized geometrical parameters of 4-Hydroxy-3-Nitrocoumarin obtained by B3LYP/ 6-31G* density functional calculations

Para meters	Bond length of 4H3NC* (Å)	Parameters	Bond angle of 4H3NC* (^{0})
O1-C2	1.4038	O1-C2-C3	114.89
C2-C3	1.4675	C2-C3-C4	121.98
C3-C4	1.3997	C3-C4-C5	119.28
C4-C5	1.4435	C4-C5-C6	117.98
C5-C6	1.4036	C5-C6-C7	120.73
C6-C7	1.3979	C6-C7-C8	118.99
C7-C8	1.3889	C7-C8-C9	121.00
C8-C9	1.4057	C8-C9-C10	119.86
C9-C10	1.3846	O1-C2-O11	116.62
C2-C11	1.2000	C3-C2-O11	128.48
C3-N12	1.4388	C2-C3-N12	118.36
C4-O13	1.3143	C4-C3-N12	119.64
C10-H14	1.0842	C3-C4-O13	124.10
C9-H15	1.0853	C5-C4-O13	116.61
C8-H16	1.0862	C9-C10-H14	121.25
C7-H17	1.0845	C8-C9-H15	120.05
N12-O18	1.2161	C10-C9-H15	120.08
N12-O19	1.2693	C7-C8-H16	119.26
O13-H20	1.0123	C9-C8-H16	119.73
		C6-C7-H17	118.91
		C8-C7-H17	122.08
		C3-N12-O18	121.02
		C3-N12-O19	117.35
		O18-N12-O19	121.62
		C4-O13-H20	105.27

* 4H3NC: 4-Hydroxy-3-Nitrocoumarin

The two possible conformers of the title compound along with labeling of atoms are shown in Fig.1. The DFT structure optimization of the title compound has shown that the conformer (b) (Fig.1) has lower energy (E = –776.746718963 a.u.) than the conformer (a) (E = –776.722215390 a.u.) for B3LYP/6-31G* method. 4-Hydroxy-3-Nitrocoumarin belongs to Cs point group symmetry. The compound has 20 atoms (Fig. 1) and hence possesses 54 fundamental modes of vibrations. For molecules of Cs symmetry, group theory analysis indicates that 54 fundamental vibrations will be distributed as: $\Gamma_{vib} = 37A'$ (in-plane) + $17A''$ (out-of-plane). From the structural point of view, 4-Hydroxy-3-Nitrocoumarin have 21 stretching vibrations, 16 in-plane bending vibrations, 8 out-of-plane bending vibrations and 9 torsion vibrations.

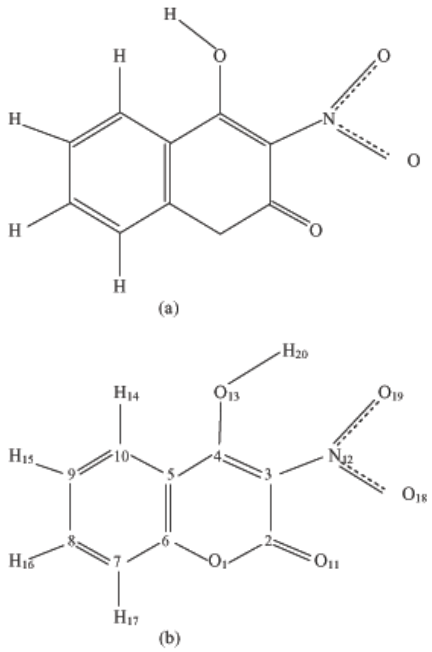

Figure 1. (a) and (b): Conformers of 4-Hydroxy-3-Nitrocoumarin along with numbering of atoms.

4.2. Assignment of Spectra

Detailed description of vibrational modes can be given by means of normal coordinate analysis. For this purpose, the full set of standard symmetry coordinates were defined as given in Table 2.

Table 2 Definition of local symmetry coordinates used in B3LYP/6-31G* force fields for 4-Hydroxy-3-Nitrocoumarin

Symmetry coordinates[a]	Description[b]
In-Plane	
$S_1 = r_{1,2} + r_{1,6}$	CO stretch
$S_2 = r_{1,2} - r_{1,6}$	CO stretch
$S_3 = r_{2,11}$	CO stretch
$S_4 = r_{4,13}$	CO stretch
$S_5 = r_{3,2} + r_{3,4}$	CC stretch
$S_6 = r_{3,2} - r_{3,4}$	CC stretch
$S_7 = r_{5,4} + r_{5,6}$	CC stretch
$S_8 = r_{5,4} - r_{5,6}$	CC stretch
$S_9 = r_{7,6} + r_{7,8}$	CC stretch
$S_{10} = r_{7,6} - r_{7,8}$	CC stretch
$S_{11} = r_{9,8} + r_{9,10}$	CC stretch
$S_{12} = r_{9,8} - r_{9,10}$	CC stretch
$S_{13} = r_{5,10}$	CC stretch
$S_{14} = r_{7,17}$	CH stretch
$S_{15} = r_{10,14}$	CH stretch
$S_{16} = r_{9,15}$	CH stretch
$S_{17} = r_{8,16}$	CH stretch
$S_{18} = r_{3,12}$	CN stretch
$S_{19} = r_{12,19}$	NO stretch
$S_{20} = r_{12,18}$	NO stretch
$S_{21} = r_{13,20}$	OH stretch
$S_{22} = \beta_{1,2,3} - \beta_{2,3,4} + \beta_{3,4,5} - \beta_{4,5,6} + \beta_{5,6,1} - \beta_{16,1,2}$	RingA def
$S_{23} = \beta_{1,2,3} - \beta_{2,3,4} - \beta_{3,4,5} + 2\beta_{4,5,6} - \beta_{5,6,1} - \beta_{6,1,2}$	RingA def
$S_{24} = \beta_{2,3,4} - \beta_{3,4,5} + \beta_{5,6,1} - \beta_{6,1,2}$	RingA def
$S_{25} = \beta_{7,6,5} - \beta_{6,5,10} + \beta_{5,10,9} - \beta_{10,9,8} + \beta_{9,8,7} - \beta_{8,7,6}$	RingB def
$S_{26} = 2\beta_{7,6,5} - \beta_{6,5,10} - \beta_{5,10,9} + 2\beta_{10,9,8} - \beta_{9,8,7} - \beta_{8,7,6}$	RingB def
$S_{27} = \beta_{6,5,10} - \beta_{5,10,9} + \beta_{9,8,7} - \beta_{8,7,6}$	RingB def
$S_{28} = \beta_{8,7,17} - \beta_{6,7,17}$	CH rock
$S_{29} = \beta_{9,8,16} - \beta_{7,8,16}$	CH rock
$S_{30} = \beta_{10,9,15} - \beta_{8,9,15}$	CH rock
$S_{31} = \beta_{5,10,14} - \beta_{9,10,14}$	CH rock
$S_{32} = \beta_{5,4,13} - \beta_{3,4,13}$	CO rock
$S_{33} = \beta_{1,2,11} - \beta_{3,2,11}$	CO rock
$S_{34} = \beta_{2,3,12} - \beta_{4,3,12}$	CN rock
$S_{35} = \beta_{3,12,18} - \beta_{3,12,19}$	NO rock
$S_{36} = \beta_{18,12,19}$	ONO bend
$S_{37} = \beta_{4,13,20}$	COH bend
Out-of-plane	
$S_{38} = \gamma_{17,7,8,6}$	CH wagg
$S_{39} = \gamma_{16,8,9,7}$	CH wagg
$S_{40} = \gamma_{15,9,10,8}$	CH wagg
$S_{41} = \gamma_{14,10,5,9}$	CH wagg
$S_{42} = \gamma_{11,2,1,3}$	CO wagg
$S_{43} = \gamma_{13,4,5,3}$	CO wagg
$S_{44} = \gamma_{12,3,2,4}$	CN wagg
$S_{45} = \gamma_{3,12,18,19}$	CN wagg
$S_{46} = \tau_{1,2,3,4} - \tau_{2,3,4,5} + \tau_{3,4,5,6} - \tau_{4,5,6,1} + \tau_{5,6,1,2} - \tau_{6,1,2,3}$	RingA tors
$S_{47} = \tau_{1,2,3,4} - \tau_{3,4,5,6} + \tau_{4,5,6,1} - \tau_{6,1,2,3}$	RingA tors
$S_{48} = -\tau_{1,2,3,4} + 2\tau_{2,3,4,5} - \tau_{3,4,5,6} - \tau_{4,5,6,1} + 2\tau_{5,6,1,2} - \gamma_{6,1,2,3}$	RingA tors
$S_{49} = \tau_{7,6,5,10} - \tau_{6,5,10,9} + \tau_{5,10,9,8} - \tau_{10,9,8,7} + \tau_{9,8,7,6} - \gamma_{8,7,6,5}$	RingB tors
$S_{50} = \tau_{7,6,5,10} - \tau_{5,10,9,8} + \tau_{10,9,8,7} - \tau_{8,7,6,5}$	RingB tors
$S_{51} = -\tau_{7,6,5,10} + 2\tau_{6,5,10,9} - \tau_{5,10,9,8} - \tau_{10,9,8,7} + 2\tau_{9,8,7,6} - \tau_{8,7,6,5}$	RingB tors
$S_{52} = \tau_{7,6,5,4} - \tau_{10,5,6,1}$	Butterfly
$S_{53} = \tau_{5,4,13,20} + \tau_{13,4,13,20}$	OH tors
$S_{54} = \tau_{4,3,12,18} + \tau_{12,3,12,18} + \tau_{4,3,12,19} + \tau_{2,3,12,19}$	NO tors

For numbering of atoms refer Figure 1.

[a] Definitions are made in terms of the standard valance coordinates:

$r_{i,j}$ is the bond length between atoms i and j;

$\beta_{I,j,k}$ is the valance angle between atoms i, j, k where j is the central atom;

$\gamma_{i,j,k,l}$ is the out-of-plane angle between the i-j bond and the plane defined by the j, k, l atoms:

$\tau_{i,j,k,l}$ is the torsional (dihedral)angle between the plane defined by the i,j,k and j,k,l atoms;
[b] stretch, def, rock, wagg, bend and tors mean stretching, deformation, rocking, wagging, bending and torsional motions, respectively,

The observed and calculated wavenumbers and normal mode descriptions for the title compound are reported in Table 3. The observed and simulated IR spectra of 4-Hydroxy-3-Nitrocoumarin are presented in Fig. 2 and the observed and simulated Raman spectra of 4-Hydroxy-3-Nitrocoumarin are presented in Fig. 3.

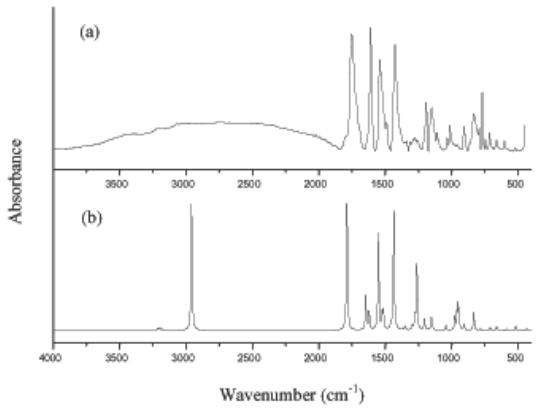

Figure 2. Comparison of observed and calculated FT-Infrared spectra of 4-Hydroxy-3-Nitro coumarin: (a) observed in solid phase; (b) calculated with B3LYP/6-31G*

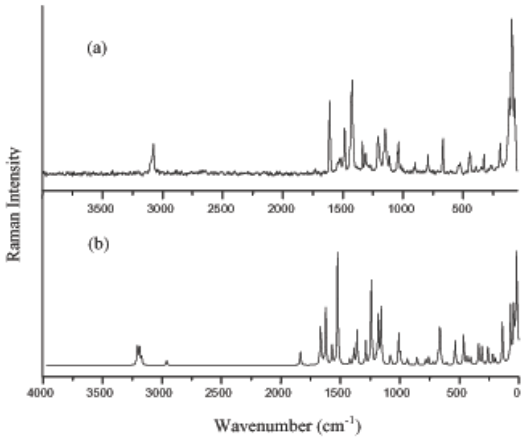

Figure 3. Comparison of observed and calculated FT-Raman spectra of 4-Hydroxy-3-Nitro coumarin: (a) observed in solid phase; (b) calculated with B3LYP/6-31G*

When using computational methods to predict theoretical normal vibrations for relatively complex polyatomics, scaling strategies are used to bring computed wavenumbers into closer agreement with observed wavenumbers. For the DFT method employed in this work the simplest limiting scaling strategy was used.

The average difference between unscaled wavenumbers and observed wavenumbers for 4-Hydroxy-3-Nitrocoumarin was approximately 12.16 cm^{-1}. In order to reproduce the observed wavenumbers, refinement of scaling factors were applied and optimized via least square refinement algorithm which resulted an average difference of 4.91 cm^{-1} between the experimental and scaled quantum mechanical (SQM) wavenumbers for 6-31G* basis set.

All vibrational assignments are based on the respective point group symmetry of the molecule. Assignments were made through visualization of the atomic displacement representations for each vibration, viewed through GAUSSVIEW [45] and matching the predicted normal wavenumbers and intensities with experimental data. It is convenient to discuss the vibrational spectra of 4-Hydroxy-3-Nitrocoumarin in terms of characteristic spectral regions as described below.

4.2.1. C–H Vibrations

Aromatic compounds commonly exhibit multiple weak band in the region 3100–3000 cm^{-1} due to aromatic C–H stretching vibrations. In the present study the weak band appears at 3081cm^{-1} in IR spectrum is assigned to C–H stretching vibrations. The Weak bands at 3118 cm^{-1}, 3093 cm^{-1}, 3080 cm^{-1} and 3025 cm^{-1} in Raman Spectrum have been assigned to C–H stretching vibrations. The C–H out-of-plane bending vibrations are strongly coupled vibrations and occur in the region 900–667 cm^{-1}. Hence, the bands appeared at 900 cm^{-1}, 800 cm^{-1}, 792 cm^{-1} in IR spectrum and 890 cm^{-1}, 810 cm^{-1}, 793 cm^{-1} in Raman spectrum of the title compound have been assigned to C–H out-of-plane bending vibrations. The in-plane and out-of-plane bending vibrations of C–H bond have also been identified for the title compound and they are presented in Table 3. They are in good agreement with the literature values [46-48].

4.2.2. C–C vibrations

Benzene has two degenerate modes, e_{2g} (1596 cm^{-1}) and e_{1u} (1485 cm^{-1}), and two non-generate modes, b_{2u} (1310 cm^{-1}) and a_{1g} (995 cm^{-1}), due to skeleton stretching of C–C bonds. Bands between 1300 cm^{-1} and 1650 cm^{-1} are assigned to C–C stretching modes. In the IR spectrum, very strong

bands at 1600 cm^{-1}, 1548 cm^{-1}, and two weak bands at 1380 cm^{-1}, 1313 cm^{-1} are assigned to C–C Stretching vibrations. In all these modes, the contributions of C–C stretching vibrations are present along with the rings' deformation. This kind of mixing of modes is a consequence of the lowering of symmetry and it has been observed in mono-substituted benzenes, nitrobenzene, phenol, benzaldehyde, azobenzenes, naphthalene, coumarin[1]. The actual positions are determined not so much by the nature of the substituents, but by the form of substitution around the ring. All the wavenumbers except that of the ring breathing mode (995 cm^{-1}) remain practically unaffected by substitution. The in-plane and out-of-plane bending vibrations of carbon atoms are found in the respective characteristic region and they are listed in Table 3.

4.2.3. C=O Vibrations

The carbonyl stretching frequency has been most extensively studied by infrared spectroscopy. Normally this multiply bonded group is highly polar and therefore gives rise to an intense infrared absorption band. The carbon-oxygen double bond is formed by Pπ–Pπ bonding between carbon and oxygen. Because of the different electro negativities of carbon and oxygen atoms the bonding electrons are not equally distributed between the two atoms. The following two resonance forms contribute to the bonding of the carbonyl group: $> C = O \leftrightarrow C^{+} - C^{-}$. The lone pair of electrons on oxygen also determine the nature of the carbonyl group. The position of the C=O stretching vibration is very sensitive to various factors, such as the physical state, electronic effects by substituents, ring strains, etc. [49]. Consideration of these factors provides further information about the environment of the C=O group. The carbonyl stretching generally occurs as a strong absorption in the region from 1730 to 1645 cm^{-1}. This portion of the infrared and Raman spectrum is most useful because the position of the carbonyl absorption is quite sensitive to substitution effects and the geometry of the molecule. In the present investigation, the peaks identified at 1871 cm^{-1} in IR spectrum and 1870 cm^{-1} in Raman spectrum have been assigned to C=O stretching vibrations. This shift in wavenumber is due to the influence of oxygen present in NO_2 group [50].

4.2.4. C–N Vibrations

C–N vibrations are identified with the help of force field calculations because, identification of C–N vibrations is a difficult task since the mixing of vibrations is possible. The unconjucated C–N linkage in the nitro give medium to weak bands near 1250 – 1020 cm^{-1} because of C–N stretching vibrations [51]. The strong peak in IR spectrum at 1018 cm^{-1} and a medium peak in Raman spectrum at 1037 cm^{-1} are assigned to C–N stretching vibrations. The bands observed in Raman spectrum at 1870 cm^{-1}, 1694 cm^{-1}, 1680 cm^{-1} and 1645 cm^{-1} have been assigned to C–N stretching modes.

4.2.5. O–H Vibrations

The O–H stretching vibrations are sensitive to hydrogen bonding. The non-hydrogen bonded or a free hydroxyl group absorb strongly in the 3550-3700 cm^{-1} region. Hydrogen bonding alters the wavenumbers of the stretching and bending vibrations. The O–H stretching bands move to lower wavenumers usually with increased intensity and band broadening in the hydrogen bonded species. In the present study, the stretching vibrations of hydrogen group were observed in Raman spectrum at 3010 cm^{-1}. This shift in the O–H stretching vibration in the title compound reflects the strength of hydrogen bond [52]. The O–H in-plane vibrations are strongly mixed with other vibrations. The strong band observed at 1489 cm^{-1} in Raman spectrum were assigned to the O–H in-plane vibration. The O–H torsional vibration is very anharmonic; therefore it is difficult to reproduce this frequency with a harmonic approach [51]. In Raman spectrum the medium band observed at 1209 cm^{-1} was assigned to torsional vibration.

4.2.6. Nitro Group vibrations

The symmetric and symmetric stretching vibrations of the nitro group are also occurring in the same C–C stretching regions. The very strong band observed in IR spectrum at 1420 cm^{-1} and at 1423 cm^{-1} in Raman spectrum are assigned to NO_2 symmetric stretching vibrations. The deformation vibrations of NO_2 group (rocking, wagging and twisting) contribute to several normal modes in the low frequency region [53]. In IR Spectrum the nitro group vibrations are observed at 780 cm^{-1}, 746 cm^{-1}, and 710 cm^{-1}. In Raman spectrum the nitro group vibrations are observed at 750 cm^{-1}, 701 cm^{-1}, 698 cm^{-1}, 449 cm^{-1}, 165 cm^{-1}, 78 cm^{-1} and 34 cm^{-1}. Based on the SQM results the strong NO_2 torsional mode can be expected to appear below 100 cm^{-1} only. In the present study calculated wavenumber 69 cm^{-1} due to torsional mode agrees will with the band at 78 cm^{-1} in Raman spectrum [54].

5. Conclusion

The DFT based SQM approach provides the most reliable theoretical information on the vibrational properties of medium-size molecules. Based on the force field obtained by density functional theory calculations at B3LYP/6-31G* level, the vibrational wavenumbers, infrared intensities and Raman activities were calculated and a complete vibrational analysis of the title compound has been carried out.

Refinement of scaling factors applied in this investigation achieved a weighted rms deviation of 4.91 cm^{-1} between the experimental and SQM wavenumbers.

Acknowledgement

The authors are thankful to Spectroscopy / Analytical test facility, Indian Institute of Science, Bangalore, and Nehru Memorial College, Puthanampatti, Tiruchirappalli, India for providing spectral measurements.

References

[1] Veenasangeeta Sortur, Jayashree Yenagi, J. Tonannavar, V.B. Jadhav, M.V. Kulkarni, Spectrochim. Acta A 64 (2006) 301–307.

[2] H. Kolancilar, U. Oyman, J. Indian Chem. Soc. 80 (2003) 853–857.

[3] R.O. Kennedy, R.D. Thomes, Coumarins: Biology, Applications and Mode of Action, Wiley, Chichester, 1997.

[4] C. Karapire, H. Kolancilar, U.Oyman, S. Icli, J. Photochem, Photobiol. A: Chem., 153 (2002) 173–184

[5] U. Joshi, R. Kelkar, M. Paradkar, Indian J. Chem. Soc. 22B (1983) 1151–1152.

[6] V. Arjunan, N. Puviarasan, S. Mohan, P. Murugesan, Spectrochim. Acta A 67 (2007) 1290-1296.

[7] G. Feuer, G.P.Ellis, G.B. West (Eds.), Progress in Medicinal Chemistry, North Holland Publishing Co., Yew York, 1974.

[8] M. Agarwal, S.B. Bansal, O.P. Singhal, J. Indian Chem. Soc. 58 (1981) 200–201.

[9] S. Shah, D. Desai, R.H. Mehta, J. Indian Chem. Soc. 76 (1999) 507-508.

[10] A.A. Deana, J. Med. Chem. 26 (1983) 580–585.

[11] T.O. Soine, J. Pharm. Sci. 53 (1964) 231–264.

[12] E. Wenkert, B. L Buckwalter, J. Am. Chem. Soc. 94 (1972) 4367-4369.

[13] R.V. Nair, E.P. Fischer, S.H. Safe, C. Courtez, R.G. Harvey, J. DiGiovanni, Carcinogenesis 12 (1991) 65–69.

[14] X. Sang, X. Shipping, L. Lanmin, Chem. Abstr. 133 (2000) p. 104942.

[15] M.K. Subramanian, P.M. Anbarasan, S. Manimegalai, Indian Academy of Sciences, 74 (2010) 845-860.

[16] S. Shah, R.H. Mehta, Indian J. Chem. 16B (1978) 704-708.

[17] M.F. Clotheir, L. Byunghyun, Chem. Abstr. 117 (1992) p. 787.

[18] M.A.A. Moustafa, Sci. Pharm. 59 (1991) p. 213.

[19] K. Yasunaka, F. Abe, A. Nagayama, H. Okabe, L. Lozada-Perez, E. Lopez-Villafranco, E.E. Muniz, A. Aguilar, R. Reyes-Chilpa, J. Ethnopharmacol, 97 (2005) 293-299.

[20] C. Shekhar, D. Lakkannuar, M.V. Kulkarni, V.P. Patil, Indian J. Chem. Soc. 69 (1992) 399-404.

[21] A.S. Gupta, M.S. Phull, J. Indian Chem. 35B (1996) p. 276.

[22] C. Ito, M. Itoigawa, S. Onada, A. Hosokawa, N. Ruangrungsi, T. Okuda, H. Tokuda, H. Nishino, H. Furukawa, Photochemistry, 66 (2005) p. 567.

[23] M.J. Maronalli, J. Chem. Phys. 106 (1997) p. 1545.

[24] R.P. Singh, J.M. Srivastava, Indian J. Chem. 26B (1987) p. 917.

[25] A. Karaliota, O. Kretsi, C. Tzougraki, J. Inorg. Biochem. 84 (2001) 33–37.

[26] A. Nagarajan, T.R. Balasubramanian, Indian J. Chem. Sect. 26B (1987) 917–919.

[27] A. Nagarajan, T.R. Balasubramanian, Indian J. Chem. Sect. 27B (1988) p. 380.

[28] R.C. Larock, E.K. Yum, M.J. Doty, K.K.C. Sham, J. Org. Chem. 60 (1995) 3270–3271.

[29] H.Y. Liao, C.H. Cheng, J. Org, Chem. 60 (1995) 3711–3716.

[30] T. Izumi, Y. Nishimoto, K. Kohi, A. Kashore, J. Heterocycl. Chem. 34 (1990) p. 2754.

[31] T. Sakamoto, M. Annaka, Y. Kondo, H. Yamanaka, Chem. Pharm. Bull., 34 (1986) 2754–2759.

[32] R.C. Larock, S. Varapath, H.H. Lau, C.A. Fellows, J. Am. Chem. Soc. 106 (1984) 5274–5284.

[33] N.V. Purohit, S.N. Mukherjee, J. Indian Chem. Soc. 75 (1998) p. 310.

[34] W.J. Hehre, L. Radom, P.V.R. Schleyer, J.A. Pople, Ab Initio Molecular Orbital Theory, John Wiley & Sons, New York, 1986.

[35] E.F. Healy, A. Holder, J. Mol. Struct. (Theochem) 281 (1993) 141–156.

[36] N.J. Harris, J. Phys. Chem. 99 (1995) 14689–14699.

[37] J.W. Finley, P.J. Stephens, J. Mol. Struct. (Theochem) 357 (1995) 225–235.

[38] M. J. Frisch, G. W. Trucks, H. B. Schlegel, G. E. Scuseria, M. A. Robb, J. R. Cheeseman, J. A. Montgomery, Jr., T. Vreven, K. N. Kudin, J. C. Burant, J. M. Millam, S. S. Iyengar, J. Tomasi, V. Barone, B. Mennucci, M. Cossi, G. Scalmani, N. Rega, G. A. Petersson, H. Nakatsuji, M. Hada, M. Ehara, K. Toyota, R. Fukuda, J. Hasegawa, M. Ishida, T. Nakajima, Y. Honda, O. Kitao, H. Nakai, M. Klene, X. Li, J. E. Knox, H. P. Hratchian, J. B. Cross, C. Adamo, J. Jaramillo, R. Gomperts, R. E. Stratmann, O. Yazyev, A. J. Austin, R. Cammi, C. Pomelli, J. W. Ochterski, P. Y. Ayala, K. Morokuma, G. A. Voth, P. Salvador, J. J. Dannenberg, V. G. Zakrzewski, S. Dapprich, A. D. Daniels, M. C. Strain, O. Farkas, D. K. Malick, A. D. Rabuck, K. Raghavachari, J. B. Foresman, J. V. Ortiz, Q. Cui, A. G. Baboul, S. Clifford, J. Cioslowski, B. B. Stefanov, G. Liu, A. Liashenko, P. Piskorz, I. Komaromi, R. L. Martin, D. J. Fox, T. Keith, M. A. Al-Laham, C. Y. Peng, A. Nanayakkara, M. Challacombe, P. M. W. Gill, B. Johnson, W. Chen, M. W. Wong, C. Gonzalez, and J. A. Pople, Gaussian 2003, Gaussian Inc.: Pittsburgh, 2003.

[39] A.D. Becke, J. Chem. Phys. 98 (1993) 5648–5652.

[40] C. Lee, W. Yang, R.G. Parr, Phys. Rev. B37 (1988), 785-789.

[41] G. Fogarasi, X.F. Zhou, P.W. Taylor, P. Pulay, J. Am. Chem. Soc. 114 (1992) 8191–8201.

[42] G. Rallhut, P. Pulay, J. Phys. Chem. 99 (1995) p. 3093.

[43] T. Sundius, J. Mol. Struct, 218 (1990) p. 321 (MOLVIB: A program for Harmonic Force Field Calculations, QCPE Program No. 604, 1991).

[44] T. Sundius, Vib. Spectrosc. 29 (2002) p. 89.

[45] V.Krishnakumar, N. Jayamani, R. Mathammal, J. Raman Spectros. 40 (2009) 936-940.

[46] E. Wille, W. Luttke. Liebigs, Ann. Chem. (1980) 2039–2054.

[47] E. Tatch, B. Schrader, J. Raman Spectros. 26 (1995) 467–473.

[48] S. Itoh, S. Ohno, N. Hasegawa, H. Takahashi, J. Raman Spectros. 20 (1989) p. 423–430.

[49] D.N. Sathyanarayana, (2^{nd} Edn.), Vibrational Spectroscopy – Theory and Applications, New Age International (P) limited, New Delhi, 2004.

[50] Y. Sheena Mary, Hema Tresa Varghese, C. Yohannan Panicker, Tugba Ertan, Ilkay Yildiz, Ozlem Temiz-Arpachi, Spectrochim. Acta A 71 (2008) 566–571.

[51] B.K. Sharma, (11^{th} Edn.), Spectroscopy, GOEL Publishing House, Meerut, 1995/1996.

[52] V. Krishnakumar, S. Muthunatesan, Spectrochim. Acta A 65 (2006) 818–825.

[53] A. Kovacs, G. Keresztury, V. Izvekov, Chem.. Phys. 253 (2000) 193–204.

[54] K. Rutkowski, A. Koll J. Mol. Struct. 322 (1994) 195-203.

Table 3

Calculated wavenumbers (cm^{-1}) of 4-Hydroxy-3-Nitrocoumarin by B3LYP/6-31G* method and vibrational assignments based on potential energy distribution (PED)

Mode No.	Symmetry Species	Observed Wavenumber (cm^{-1})		Calculated wavenumber (cm^{-1}), B3LYP/6-31G* force field				Characterization of normal modes with PED(%)
		IR	Raman	Unscaled	Scaled	IR[a] Intensity	Raman[b] activity	
Q1	A'	-	3118 vw	3116	3114	5.024	127.143	νCH(99)
Q2	A'	-	3093 vw	3099	3080	1.551	124.510	νCH(99)
Q3	A'	3081 vw	3080 vw	3081	3078	9.342	165.443	νCH(99)
Q4	A'	-	3025 vw	3028	3024	3.686	79.143	νCH(99)
Q5	A'	-	3010 s	2984	2988	477.862	38.862	νOH(100)
Q6	A'	1871 vw	1870 vw	1867	1862	538.669	36.213	νCO(62), bCN(11), bRingA (11), νCC(8), ωCN(7)
Q7	A'	-	1694 vw	1673	1694	108.192	77.192	ωCN(31), νCC(31), bRingA(8), bCN(7), νCO(5)
Q8	A'	-	1680 vw	1655	1685	405.254	29.914	νCC(35), ωCN(17), bCN(14), bRingA(11), νCO(8), bRingB(6)
Q9	A'	-	1645 vw	1648	1651	47.447	119.539	νCC(52), ωCN(19), bRingB(7), bCH(6)
Q10	A'	1600 vs	1601 vs	1598	1596	231.196	37.897	νCC(50), bCN(12), ωCN(11), bCH(6)
Q11	A'	1548 vs	1545 m	1539	1550	367.196	210.237	νCC(31), νCO(17), bRingA(14), bCN(12), bCOH(8), bCO(6)
Q12	A'	1489 s	1485 s	1498	1481	41.655	1.762	νCC(41), bCH(27), bCOH(16)
Q13	A'	-	1464 m	1491	1449	31.017	9.182	νCC(44), νCO(22), bCH(14), bCN(8)
Q14	A'	1420 vs	1423 vs	1397	1415	13.506	25.402	νCC(38), bCOH(14), bCH(10), bRingA (9), νCO(8), νNO(7)
Q15	A'	1380 vw	1380 vw	1384	1387	24.902	53.621	νCC(84)
Q16	A'	1313 w	1315 m	1312	1314	42.064	33.323	νCC(30), νCO(15), bCN(10), νNO(9), ωCN(7), bCOH(6)
Q17	A'	1270 w	1271 w	1300	1267	214.193	112.673	tOH(19), νCC(18), νCO(16), bCOH(9), νCN(8), bCO(7)
Q18	A'	1258 w	-	1249	1254	42.403	2.585	bCH(49), ωCN(10), bRingA(10), bCN(8), νCO(6), νCC(6)
Q19	A'	-	1235 vw	1224	1227	172.260	7.847	νCC(33), νCN(16), νCO(13), bRingA(11), tOH(6), bCH(5)
Q20	A'	-	1209 m	1213	1209	93.571	59.342	tOH(35), νCO(17), νCC(14), ωCN(11), bCN(7), νNO(5)
Q21	A'	1192 vs	-	1181	1185	51.381	67.429	νCC(21), bCH (17), νCO(15), bCN(13), bRingB(11), tOH(9)
Q22	A'	1111 s	1115 w	1140	1108	4.151	9.666	bCH(88), νCC(10)
Q23	A'	-	1091 vw	1061	1098	17.866	3.507	bCH(61), νCC(19), bRingB(14)

Q24	A"	1034 w	1048 w	999	1037	7.815	29.922	νCC(44), bCH(34), νCO(7), bCN(5)
Q25	A'	1018 s	1037 m	993	1023	2.080	9.793	νCO(22), ωCH(20), νCN(11), νCC(9), bCO(7), bCN(6)
Q26	A"	-	1004 vw	972	997	1.588	0.750	ωCH(6), tRingB (8)
Q27	A'	-	978 vw	928	972	4.319	0.927	ωCH(80), tRingB(9)
Q28	A'	960 vw	966 vw	909	963	85.173	5.285	bCN(26), νCO(22), ωCN(15), bCO(14), ωCH(8), νCC(7)
Q29	A"	-	943 vw	908	933	26.046	0.566	bRingB(8), νCO(18), bRingA(11), νCC(8), bCO(5)
Q30	A"	870 s	890 w	885	882	18.033	5.923	ωCH(26), νCC(10), bCNO(8), νNO(8), tRingB(7), bCN(6)
Q31	A'	800 s	810 m	797	808	30.090	3.581	ωCH(32), ωCN(17), tRingB(13), bCNO(8), νNO(7), bRingA(6)
Q32	A"	792 s	793 m	785	787	49.500	2.681	ωCH(29), bCNO(16), νNO(11), tRingB(9), ωCO(8), ωCN(7)
Q33	A"	780 vs	-	755	784	15.301	2.558	tRingA(30), ωCN(22), tNO2(19), ωCO(10), tRingB(10), bCNO(6)
Q34	A"	746 m	750 vw	748	747	2.459	1.829	ωCO(33), tRingA(23), tNO2(17), ωCN(14), tRingB(6)
Q35	A"	710 m		704	708	4.619	3.915	tRingB(48), tNO2(20), ωCN(6), bRingB(5)
Q36	A'	-	701 vw	683	695	2.109	7.662	tRingB(48), tNO2(20), ωCN(6), bRingB(5)
Q37	A'	-	698 w	674	693	4.164	8.448	tNO2(25), bRingB(12), bRingA(11), bCNO(9), tRingB(8), ωCH(7)
Q38	A"	-	690 s	667	687	4.643	12.351	tRingA(29), ωCO(20), ωCH(10), tRingB(10), tNO2(5)
Q39	A'	-	636 m	609	635	10.939	1.148	bRingB(28), bRingA(25), νCN(13), νCC(11), ωCN(7), bCO(5)
Q40	A'	580 m	570 vw	536	561	0.530	9.565	bRingA(38), bRingB(23), νCC(20), νCO(10)
Q41	A"	-	539 w	534	533	0.874	0.507	tRingB(62), ωCH(11), tRingA(8)
Q42	A'	510 w	-	451	490	11.312	9.707	bRingA (52), bRingB(14), νCC(13), bCO(7), bCN(7)
Q43	A'	-	470 w	443	460	2.257	2.268	ωCN(38), bCNO(28), bCN(8), bCO(7), νNO(7)
Q44	A"	-	449 m	440	446	4.673	0.582	tRingB(36), ωCN(17), tNO2(6), ωCH(5)
Q45	A'	-	442 vw	405	432	7.163	1.935	bCO(28), bCNO(18), νNO(14), νCC(10), νCO(7), bRingA(5)
Q46	A'	-	380 vw	356	366	1.304	4.377	bCN(43), νCN(12), νCO(9), bRingA(8), νCC(8), ωCN(7)
Q47	A'	-	348 vw	324	336	2.185	3.326	bCN(34), ωCN(11), bCNO(10), bRingB(9), νCC(9), bRingA(8)
Q48	A"	-	300 m	278	287	3.806	2.486	ωCN(52), tRingA(11), tRingB(10), bCNO(8)
Q49	A"	-	260 vw	250	246	4.785	1.117	ωCN(51), tRingA(26), bCNO(9), tRingB(6)
Q50	A'	-	230 m	226	222	0.206	0.549	bCNO(33), ωCN(23), bCN(21), νNO(12)

Q51	A"	-	165 vw	163	164	0.167	2.349	tRingA(44), ωCN(25), tNO2(11), bCNO(7), tRingB(5)
Q52	A"	-	103 vs	91	96	0.230	1.203	νNO(37), bONO(23), bCNO(13), tRingA(11), tNO2(8)
Q53	A"	-	78 s	76	69	0.369	0.526	νNO(30), tRingA(27), bONO(23), tNO2(7)
Q54	A"	-	34 vw	31	31	0.114	2.471	νNO(36), bONO(35), tRingA(17), bCNO(12)

Abbreviations: ν: stretching; b: bending; ω: wagging; t: torsion s-strong; vs-very strong; w-weak; m-medium ; vw-very weak.
[a] Relative absorption intensities normalized with highest peak absorption.
[b] Relative Raman intensities calculated by Eqn.(2).